

# Training-free Long Video Generation with Chain of Diffusion Model Experts

Wenhao Li<sup>1\*</sup>†, Yichao Cao<sup>2\*</sup>, Xiu Su<sup>3‡</sup>, Xi Lin<sup>4</sup>, Shan You<sup>5</sup>, Mingkai Zheng<sup>1</sup>, Yi Chen<sup>6</sup>, Chang Xu<sup>1</sup>

<sup>1</sup>University of Sydney, <sup>2</sup>Southeast University, <sup>3</sup>Central South University, <sup>4</sup>Shanghai Jiaotong University, <sup>5</sup>Sensetime Research, <sup>6</sup>Hong Kong University of Science and Technology

## Abstract

Video generation models hold substantial potential in areas such as filmmaking. However, current video diffusion models need high computational costs and produce suboptimal results due to high complexity of video generation task. In this paper, we propose **ConFiner**, an efficient high-quality video generation framework that decouples video generation into easier subtasks: structure **control** and spatial-temporal **refinement**. It can generate high-quality videos with chain of off-the-shelf diffusion model experts, each expert responsible for a decoupled subtask. During the refinement, we introduce coordinated denoising, which can merge multiple diffusion experts' capabilities into a single sampling. Furthermore, we design ConFiner-Long framework, which can generate long coherent video with three constraint strategies on ConFiner. Experimental results indicate that with only 10% of the inference cost, our ConFiner surpasses representative models like Lavie and Modelscope across all objective and subjective metrics. And ConFiner-Long can generate high-quality and coherent videos with up to 600 frames. All the code will be available at project website: <https://confiner2025.github.io>.

## Introduction

Generative AI (Cao et al. 2023; Zhang et al. 2023a; Wu et al. 2023) has recently emerged as a hotspot in research, influencing various aspects of our daily life. For visual AIGC, numerous image generation models, such as Stable Diffusion (Rombach et al. 2022) and Imagen (Saharia et al. 2022), have achieved significant success. These models can create high-resolution images that are rich in creativity and imagination, rivaling those created by human artists. Compared to image generation, video generation models (Ho et al. 2022c,a; Xing et al. 2023; Esser et al. 2023) hold higher practical value with the potential to reduce expenses in the fields of filmmaking and animation.

However, current video generation models are still in their early stages of development. Existing video diffusion models can primarily be categorized into three types. The first type uses T2I (Text to Image) models to generate videos directly without further training (Khachatryan et al. 2023). The second type incorporates a temporal module into T2I

models and trains on video datasets (Wang et al. 2023b; Blattmann et al. 2023; Lin and Yang 2024). The third type is trained from scratch (Ma et al. 2024). Regardless of which type, these methods use a single model to undertake the entire task of video generation. However, video generation is an extremely intricate task. After our in-depth analysis, we believe that this complex task consists of three subtasks: modeling the *video structure*, which includes designing the overall visual structure and plot of the video; generating *spatial details*, ensuring that each frame is produced with sufficient clarity and high aesthetic score; and producing *temporal details*, maintaining consistency and coherence between frames to ensure natural and logical transitions. Therefore, relying on a single model to handle such a complex and multidimensional task is challenging.

Overall, there are three main challenges in the current field of video generation. 1) The quality of the generated videos is low, hard to achieve high-quality temporal and spatial modeling simultaneously. 2) The generation process is time-consuming, often requiring hundreds of inference steps. Utilizing a single model to handle complex video generation task is one of the key reasons for these two issues. 3) The length of the generated videos are typically short. Due to limitations in VRAM, the length of videos generated in a single attempt generally ranges between only 2-3 seconds.

In order to enhance generation quality, some methods employ multiple models on different resolutions or in different spaces to perform progressive generation. Methods like Imagen Video (Ho et al. 2022b) and I2VGen-XL (Zhang et al. 2023c) train several diffusion models on gradually increasing resolutions to first generate a video of low resolution, and then progressively scale up. Show-1 (Zhang et al. 2023b) trains a model in pixel space to generate low-quality videos, followed by a latent space model to enhance quality. Compared to methods using a single model, these approaches achieve higher performance. However, each model still needs to handle both spatial and temporal modeling in generation. This leaves each model still heavily burdened.

To improve quality of videos while reducing inference time, we rethink the demands of video generation tasks, which include modeling video structure, generating spatial details, and producing temporal details. We find out that a more rational approach is utilizing three specialized models, each handling one demand. By doing so, these mod-

\*Equal contribution

†Email: wenhaol@buaa.edu.cn

‡corresponding author

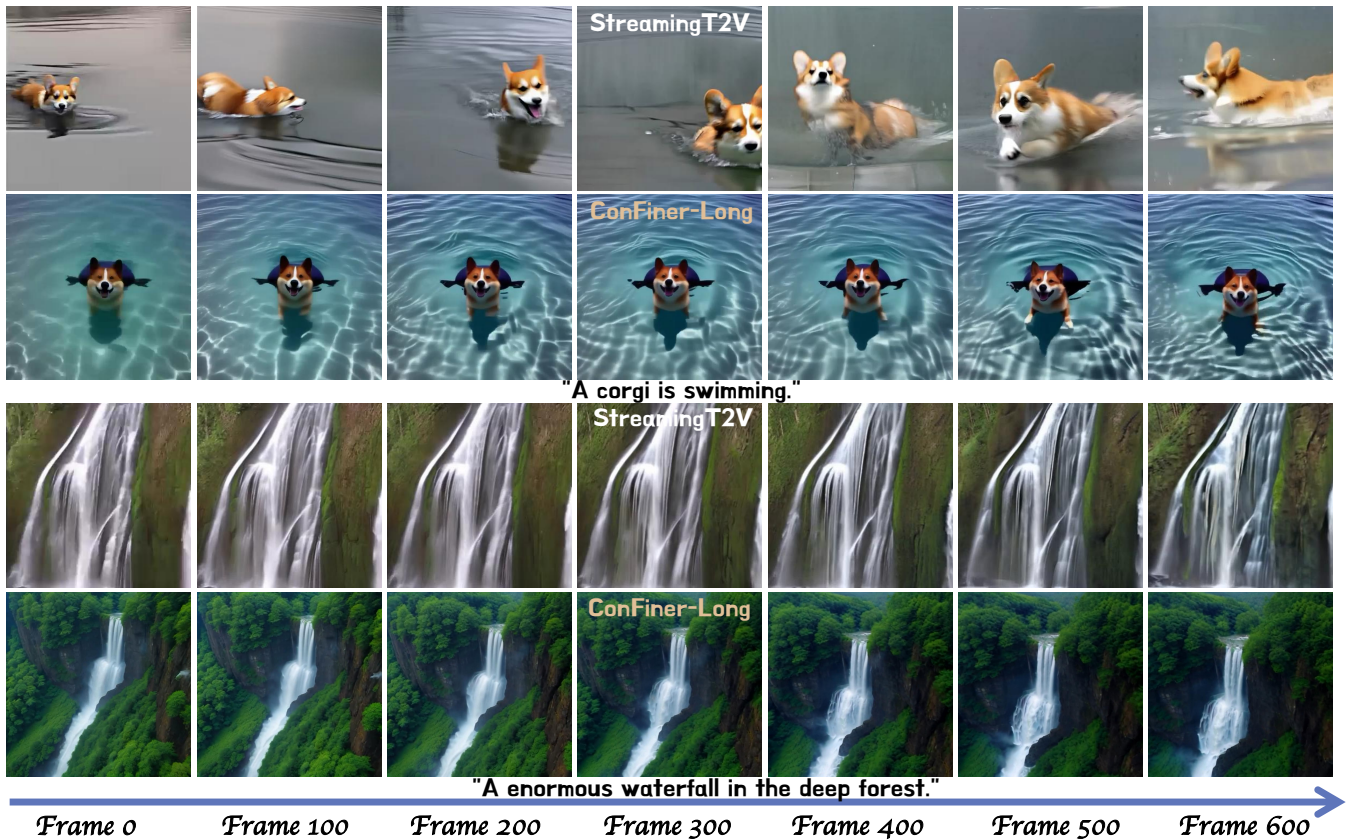


Figure 1: Visual Comparison between Our ConFiner-Long and StreamingT2V.

els can collaboratively accomplish the comprehensive task of video generation. To this end, we propose a framework named ConFiner, which decouples the video generation process into three parts: structure control, temporal refinement, and spatial refinement. During generation, we employ chain of three ready-made diffusion experts, each specializing in their respective tasks. In the control stage, a highly controllable T2V (Text to Video) model is employed as control expert, tasked with structure control. During the refinement stage, a T2I model and a T2V model skilled at generating details are employed as spatial and temporal experts to refine details. This framework can reduce the burden on individual models, enhancing both the quality and speed of generation. Moreover, as it utilizes ready-made diffusion experts, this framework does not incur additional training costs.

Moreover, during refinement stage, to enable simultaneous use of spatial and temporal experts within a single denoising process, we proposed coordinated denoising. Due to the varying noise schedulers employed by different diffusion experts, their noise distributions differ. Therefore, they cannot be directly combined during generation. In coordinated denoising, we build a bridge between the noise schedulers of two experts, enabling the collaboration of two diffusion models at the granularity of timesteps.

In terms of increasing video lengths, some methods (Wang, Li, and Chen 2024; Wang et al. 2023a; Qiu et al.

2023; Gu et al. 2023) propose generating video segments and then stitching them together to create longer videos. They use techniques such as noise control to ensure consistency between segments. Although these methods can produce extended videos within limited VRAM, the transitions between segments tend to be abrupt.

Therefore, based on ConFiner, we propose ConFiner-Long framework with three strategies to ensure the coherence and consistency between segments. As the initial noise significantly impacts the final videos, we first introduce a segments consistency initialization strategy to ensure the consistency of the initial noise between segments by sharing a base noise. Additionally, in order to enhance the coherence of the motion trend between segments, we propose a coherence guidance strategy that uses the gradient of noise differences between two segments to guide the denoising direction. Also, to address the problem of flickering at the junctions of segments, we design a staggered refinement strategy that staggers the control stage and the refinement stage. It places the tail of one video structure and the head of the next into the same refinement process to achieve more natural transitions between segments.

Experimental results have shown that ConFiner requires only 9 sampling steps (less than 5 seconds) to surpass the performance of models like AnimateDiff-Lightning (Lin and Yang 2024), LaVie (Wang et al. 2023c), and ModelScope

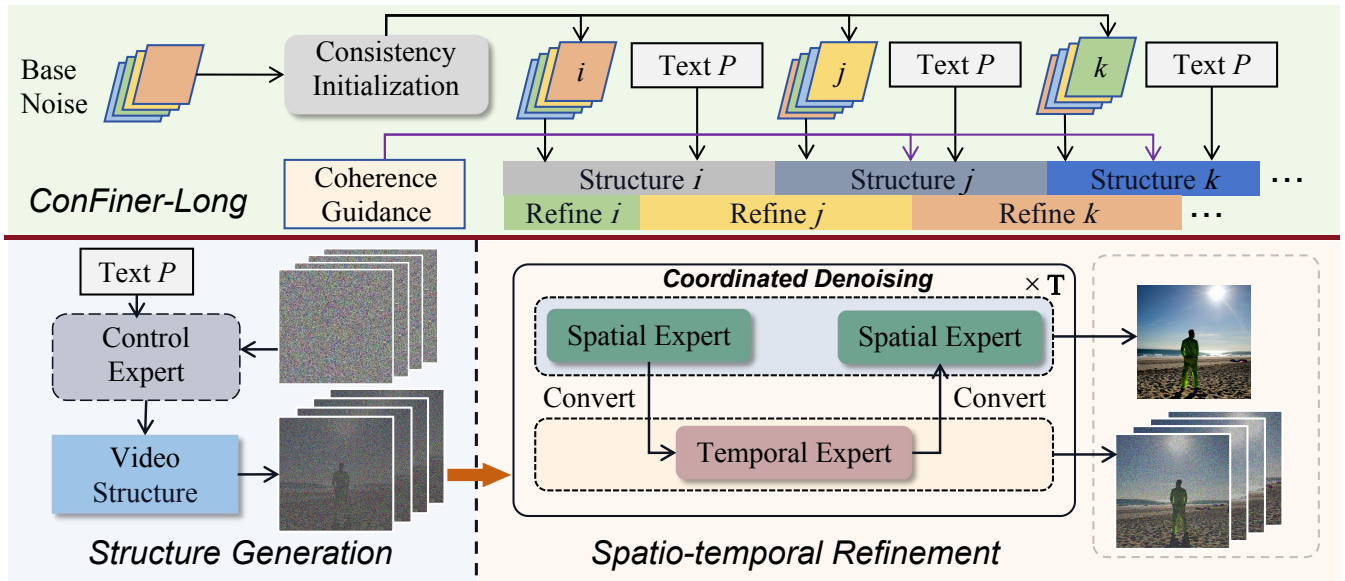


Figure 2: **Pipeline of Our ConFiner and ConFiner-Long.** ConFiner decouples the video generation process. Firstly, control expert generates a video structure. Subsequently, temporal and spatial experts perform the refinement of spatio-temporal details. Spatial and temporal experts work together in refinement stage with our coordinated denoising. By adding consistency initialization, coherence guidance and staggered refinement to ConFiner, ConFiner-Long can generate coherent long videos.

T2V (Wang et al. 2023b) with 100-step sampling (more than 1 minute) in all metrics. Furthermore, ConFiner-Long can generate high-quality coherent videos up to 600 frames long. To sum up, our contributions are as follows:

1. We introduced ConFiner, which decouples the video generation task into three sub-tasks. It utilizes three ready-made diffusion experts, each handling its specialized task. This approach reduces the model’s burden, enhancing the quality and speed of generation.
2. We developed coordinated denoising, allowing two experts on different noise schedulers to collaborate timestep-wise in video generation process.
3. We proposed ConFiner-Long framework, building on the ConFiner with three strategies to achieve high-quality, coherent long video production.

## Related Work

**Diffusion models (DMs).** DMs have achieved remarkable successes in the generation of images (Nichol and Dhariwal 2021), music (Mittal et al. 2021), and 3D models (Poole et al. 2022; Lin et al. 2023). These models typically involve thousands of timesteps, controlled by a scheduler that manages the noise level at each step. Diffusion models consist of two processes. In the forward process, noise is progressively added to the original data until it is completely transformed into noise. During the reverse denoising process, the model starts with random noise and gradually eliminates the noise using a denoising model, ultimately transforming it into a sample that matches the target distribution.

**Video Diffusion Models (VDMs).** Compared to the success of diffusion models in image generation and other areas,

VDMs are still at a very early stage. Models like text2video-zero (Khachatryan et al. 2023) that use stable diffusion without additional training for direct video generation suffer from poor coherence and evident visual tearing. Models like SVD (Blattmann et al. 2023) and Modelscope T2V (Wang et al. 2023b) convert the U-Net of stable diffusion (Wang et al. 2023c) into a 3D U-Net through the addition of temporal convolution or attention, and train it on video datasets to achieve video generation. Although these video generation models each have their strengths, none fully satisfy all the demands of video generation, such as coherence and clarity.

## Method

### Overview

Our ConFiner consists of two stages: the control stage and the refinement stage. In the control stage, it generates a video structure containing coarse-grained spatio-temporal information, which determines the overall structure and plot of the final video. During the refinement stage, it refines spatial and temporal details based on video structure. In this stage, we propose coordinated denoising to enable cooperation of spatial expert and temporal expert. Based on ConFiner, we introduce ConFiner-Long framework for producing coherent and consistent long videos.

### Revisiting Diffusion Models

The workflow of diffusion models consists of two processes: the forward process and the reverse denoising process. The forward process from timestep 0 to timestep  $t$  can be expressed as follows:

$$\mathbf{x}_t = \sqrt{\bar{\alpha}_t} \mathbf{x}_0 + \sqrt{1 - \bar{\alpha}_t} \epsilon \quad (1)$$

---

**Algorithm 1: ConFiner (Control + Refinement)**


---

```

1: Input: Prompt  $P$ , Control Expert  $C_{con}$ , Spatial Expert
    $S$ , Temporal Expert  $T$ , Noisy timestep  $T_e$ 
2: Output: Generated video  $\mathcal{V}$ 
3: // Control Stage
4:  $\mathcal{V}_0 \leftarrow \text{Generate}(P, C_{con})$ 
5:  $\text{Video\_Structure} \leftarrow \text{Add noise}(\mathcal{V}_0, T_e, C_{con})$ 
6: // Refinement Stage
7:  $\mathcal{V}'_{T_e} \leftarrow \text{Video\_Structure}$ 
8: for each refinement step  $T_k$  do
9:   if Standard Denoising then
10:     $\mathcal{V}'_{T_{k-1}} \leftarrow \text{Denoise}(\mathcal{V}'_{T_k}, T_k, S)$ 
11:   else if Coordinated Denoising then
12:     $\mathcal{V}'_0(T_k) \leftarrow \text{Denoise}(\mathcal{V}'_{T_k}, T_k, S, P)$ 
13:     $\mathcal{V}''_{T_k} \leftarrow \text{Add noise}(\mathcal{V}'_0(T_k), T_k, T)$ 
14:     $\mathcal{V}''_0(T_k) \leftarrow \text{Denoise}(\mathcal{V}''_{T_k}, T_k, T, P)$ 
15:     $\mathcal{V}'_{T_k} \leftarrow \text{Add noise}(\mathcal{V}''_0(T_k), T_k, S)$ 
16:     $\mathcal{V}'_{T_{k-1}} \leftarrow \text{Denoise}(\mathcal{V}'_{T_k}, T_k, S, P)$ 
17:   end if
18: end for
19: Return  $\mathcal{V} = \mathcal{V}'_0$ 

```

---

where  $\alpha_t = 1 - \beta_t$ ,  $\bar{\alpha}_t = \prod_{i=1}^t \alpha_i$ ,  $t$  is the diffusion step,  $\epsilon$  is a random noise sampled from Standard Gaussian Distribution  $\mathcal{N}(0, 1)$  and  $\beta_t$  is a small positive constant between 0 and 1, representing the noise level of each timestep.

During the reverse denoising process, starting from a random noise at timestep  $T$ , the denoising model progressively predicts  $\mathbf{x}_{t-1}$  from  $\mathbf{x}_t$ , ultimately getting the target data  $\mathbf{x}_0$ . Taking DDIM (Song, Meng, and Ermon 2020) as an example, the denoising model initially uses  $\mathbf{x}_t$  to predict the noise. Then,  $\mathbf{x}_t$  and the predicted noise are utilized together to compute a prediction of  $\mathbf{x}_0$  via the following expression:

$$\hat{\mathbf{x}}_0 = \frac{\mathbf{x}_t - \sqrt{1 - \bar{\alpha}_t} \epsilon_\theta^{(t)}(\mathbf{x}_t)}{\sqrt{\bar{\alpha}_t}} \quad (2)$$

where  $\epsilon_\theta^{(t)}(x_t)$ ,  $\hat{\mathbf{x}}_0$  represents the predicted noise and  $\mathbf{x}_0$ .

Then, based on the predicted noise and  $\hat{\mathbf{x}}_0$ , a prediction for  $\mathbf{x}_{t-1}$  is derived using the following expression:

$$\mathbf{x}_{t-1} = \sqrt{\bar{\alpha}_{t-1}} \cdot \hat{\mathbf{x}}_0 + \sqrt{1 - \bar{\alpha}_{t-1}} \epsilon_\theta^{(t)}(\mathbf{x}_t) \quad (3)$$

By combining eq. (2) and eq. (3), single-step denoising can be expressed as:

$$\hat{\mathbf{x}}_0, \mathbf{x}_{t-1} = \text{Denoising}(\theta, \mathbf{x}_t, t, S) \quad (4)$$

where  $S$  denotes the noise scheduler of this diffusion model and  $\theta$  represents the corresponding denoising model.

### Video Structure Generation

In the control stage, we select a video diffusion model skilled at handling video structure and employ it as control expert. The scheduler used in this expert can be denoted as  $S_{con}$ . During inference, to reduce computational overhead, we opt for a DDIM scheduler with a total inference step of  $T_{i_1}$ . When conducting inference, the list of timesteps utilized

is:  $[t_1(i_1), t_2(i_1), \dots, t_{T_{i_1}}(i_1)]$ . The selection of timesteps is made at uniform intervals.

After obtaining the timesteps list, we start with a random noise  $\mathcal{V}_{t_{T_{i_1}}(i_1)}$  and progressively perform denoising over these timesteps, getting the first version of the video  $\mathcal{V}_0$ . Single-step sampling from eq. (4) can be rewritten as follows.

$$\hat{\mathcal{V}}_0(t_k(i_1)), \mathcal{V}_{t_{k-1}(i_1)} = \text{Denoising}(\theta_{con}, \mathcal{V}_{t_k(i_1)}, t_k(i_1), S_{con}) \quad (5)$$

where  $\hat{\mathcal{V}}_0(t_k(i_1))$  represents the predicted  $\mathcal{V}_0$  at timestep  $t_k(i_1)$ ,  $\mathcal{V}_{t_k(i_1)}$  denotes  $\mathcal{V}$  at timestep  $t_k(i_1)$ ,  $\theta_{con}$  represents control expert and  $S_{con}$  is the scheduler of control expert.

While we completed the entire sampling process to obtain the first version of video  $\mathcal{V}_0$ , the quality and coherence of the video are compromised due to our choice of a small  $T_{i_1}$ .

Therefore, we introduce  $T_e$  steps of noise to  $\mathcal{V}_0$ . This operation is intended to create refinement opportunities for spatial and temporal experts. In this noise addition process, we utilize the Scheduler  $S_s$  from the spatial expert used in refinement stage, resulting in the noisy video  $\mathcal{V}'_{T_e}$  at timestep  $T_e$ . Transformed from eq. (1), this noise addition process can be expressed as:

$$\mathcal{V}'_{T_e} = \sqrt{\bar{\alpha}_{T_e}(S_s)} \cdot \mathcal{V}_0 + \sqrt{1 - \bar{\alpha}_{T_e}(S_s)} \cdot \epsilon \quad (6)$$

where  $\bar{\alpha}_{T_e}(S_s)$  is the  $\bar{\alpha}_t$  in scheduler  $S_s$  at timestep  $T_e$ .

### Spatial and Temporal Details Refinement

During the refinement stage, we add spatial and temporal details with spatial expert and temporal expert in the process of transforming  $\mathcal{V}'_{T_e}$  to  $\mathcal{V}'_0$ . Similar to the control stage, we select  $T_{i_2}$  steps for sampling between timestep  $T_e$  and timestep 0. The list of timesteps used is:  $[t_1(i_2), t_2(i_2), \dots, t_{T_{i_2}}(i_2)]$ .

Given that two experts respectively excel in spatial and temporal modeling, we aim to synergistically utilize both experts in the process of denoising  $\mathcal{V}'_{T_e}$  to  $\mathcal{V}'_0$ , thus enhancing the spatio-temporal detail. A straightforward approach is alternating between the two experts at each timestep, leveraging the strengths of both models concurrently. In this case, eq. (4) can be rewritten as follows:

$$\hat{\mathcal{V}}_0(t_k(i_2)), \mathcal{V}'_{t_{k-1}(i_2)} = \text{Denoising}(\theta_X, \mathcal{V}'_{t_k(i_2)}, t_k(i_2), S_s) \quad (7)$$

$$\text{where } \theta_X = \begin{cases} \theta_S & \text{if } k \equiv 2 \pmod{0} \\ \theta_T & \text{if } k \equiv 2 \pmod{1} \end{cases}$$

where  $\theta_S$  and  $\theta_T$  represent spatio expert and temporal expert, and  $S_s$  denotes the noise scheduler of spatial expert.

However, this method is ineffective because spatial expert and temporal expert are often on different noise scheduler. The data distributions for the spatial and temporal experts at the same timestep are inconsistent. The original data is on the scheduler of spatial expert, and directly switching to the scheduler of temporal expert at a certain timestep leads to conflicts and inconsistencies. To transform  $\mathcal{V}'_{t_k(i_2)}$  to  $\mathcal{V}'_{t_{k-1}(i_2)}$ , we provide two options.

Table 1: **Objective Evaluation Results.** In this experiment, ConFiner utilized AnimateDiff\_Lightning as the control expert and selected stable diffusion 1.5 for spatial expert. Lavie and Modelscope T2V are chosen as temporal expert.

Method	Inference Steps	Subject Consistency $\uparrow$	Motion Smoothness $\uparrow$	Aesthetic Quality $\uparrow$	Imaging Quality $\uparrow$
Lavie	10	0.940 $\pm$ 0.001	0.967 $\pm$ 0.001	0.570 $\pm$ 0.003	0.658 $\pm$ 0.008
Lavie	20	0.954 $\pm$ 0.002	0.966 $\pm$ 0.002	0.587 $\pm$ 0.001	0.683 $\pm$ 0.001
Lavie	50	0.958 $\pm$ 0.004	0.965 $\pm$ 0.006	0.597 $\pm$ 0.005	0.696 $\pm$ 0.005
Lavie	100	0.957 $\pm$ 0.003	0.965 $\pm$ 0.001	0.596 $\pm$ 0.006	0.695 $\pm$ 0.007
AnimateDiff_Lightning	10	0.983 $\pm$ 0.002	0.983 $\pm$ 0.001	0.635 $\pm$ 0.002	0.689 $\pm$ 0.001
AnimateDiff_Lightning	20	0.984 $\pm$ 0.002	0.980 $\pm$ 0.002	0.636 $\pm$ 0.006	0.697 $\pm$ 0.002
AnimateDiff_Lightning	50	0.981 $\pm$ 0.000	0.971 $\pm$ 0.000	0.638 $\pm$ 0.002	0.705 $\pm$ 0.003
AnimateDiff_Lightning	100	0.977 $\pm$ 0.004	0.964 $\pm$ 0.003	0.623 $\pm$ 0.006	0.699 $\pm$ 0.005
Modelscope T2V	10	0.983 $\pm$ 0.002	0.980 $\pm$ 0.001	0.570 $\pm$ 0.002	0.670 $\pm$ 0.004
Modelscope T2V	20	0.985 $\pm$ 0.001	0.980 $\pm$ 0.000	0.575 $\pm$ 0.003	0.702 $\pm$ 0.004
Modelscope T2V	50	0.988 $\pm$ 0.002	0.990 $\pm$ 0.001	0.592 $\pm$ 0.004	0.716 $\pm$ 0.002
Modelscope T2V	100	0.987 $\pm$ 0.002	0.990 $\pm$ 0.000	0.594 $\pm$ 0.001	0.715 $\pm$ 0.004
<b>ConFiner w/ Lavie</b>	9	0.993 $\pm$ 0.000	0.991 $\pm$ 0.000	0.699 $\pm$ 0.005	0.734 $\pm$ 0.005
<b>ConFiner w/ Lavie</b>	18	0.993 $\pm$ 0.002	0.990 $\pm$ 0.001	0.703 $\pm$ 0.009	0.739 $\pm$ 0.004
<b>ConFiner w/ Modelscope</b>	9	0.994 $\pm$ 0.001	0.991 $\pm$ 0.000	0.698 $\pm$ 0.006	0.731 $\pm$ 0.003
<b>ConFiner w/ Modelscope</b>	18	<b>0.994 <math>\pm</math> 0.000</b>	<b>0.991 <math>\pm</math> 0.002</b>	<b>0.707 <math>\pm</math> 0.004</b>	<b>0.739 <math>\pm</math> 0.004</b>

**Option 1 (Standard Denoising):** Since the original data  $\mathcal{V}'_{T_e}$  is on the scheduler of spatial expert, we can directly employ the spatial expert for denoising at time step  $t_k(i_2)$ :

$$\hat{\mathcal{V}}_0(t_k(i_2)), \mathcal{V}'_{t_{k-1}(i_2)} = \text{Denoising}(\theta_S, \mathcal{V}'_{t_k(i_2)}, t_k(i_2), S_s) \quad (8)$$

**Option 2 (Coordinated Denoising):** Although two experts' schedulers differ, both schedulers share the same distribution at timestep 0. Hence, we can utilize timestep 0 to establish a connection between the two schedulers, facilitating the concurrent use of two experts within the same timestep. The specific details of this process are as follows.

First, at timestep  $t_k(i_2)$ , given  $\mathcal{V}'_{t_k(i_2)}$ , we employ the spatial expert for a one-step inference as eq. (8). After obtaining the predicted  $\hat{\mathcal{V}}_0(t_k(i_2))$ , it can be converted to  $\mathcal{V}''_{t_k(i_2)}$  on the scheduler of temporal expert.

$$\mathcal{V}''_{t_k(i_2)} = \sqrt{\bar{\alpha}_{t_k(i_2)}(S_t)} \cdot \hat{\mathcal{V}}_0(t_k(i_2)) + \sqrt{1 - \bar{\alpha}_{t_k(i_2)}(S_t)} \cdot \epsilon \quad (9)$$

where  $S_t$  represents the noise scheduler of temporal expert.

Then we can employ the temporal expert for denoising:

$$\hat{\mathcal{V}}_0(t_k(i_2)), \mathcal{V}''_{t_{k-1}(i_2)} = \text{Denoising}(\theta_T, \mathcal{V}''_{t_k(i_2)}, t_k(i_2), S_t) \quad (10)$$

This version of  $\hat{\mathcal{V}}_0(t_k(i_2))$  predicted by temporal expert contains richer temporal information and demonstrates enhanced inter-frame coherence. Subsequently, we transform  $\hat{\mathcal{V}}_0(t_k(i_2))$  using the scheduler of spatial expert into a  $\mathcal{V}'_{t_k(i_2)}$  with more extensive temporal information.

$$\mathcal{V}'_{t_k(i_2)} = \sqrt{\bar{\alpha}_{t_k(i_2)}(S_s)} \cdot \hat{\mathcal{V}}_0(t_k(i_2)) + \sqrt{1 - \bar{\alpha}_{t_k(i_2)}(S_s)} \cdot \epsilon \quad (11)$$

Finally, the spatial expert is used again to predict  $\mathcal{V}'_{t_{k-1}(i_2)}$  including augmented spatio-temporal information as eq. (8).

### ConFiner-Long Framework

We also leverage ConFiner to design a pipeline for long video generation. This pipeline generate multiple short video segments and introduces three strategies to ensure consistency and coherence between these segments.

First, we design consistency initialization strategy to promote consistency between segments. The initial noise affects the content of the generated video significantly. To improve the consistency between segments, we first sample a  $Noise\_base \in \mathbf{R}^{H \times W \times C \times F}$ , which is then subjected to frame-wise shuffling to obtain the initial noise for each segment. Sharing base noise enhances the content consistency between segments while shuffling maintains a little randomness.

Additionally, we introduce a staggered refinement mechanism to further improve the overall coherence of the video. In our segmented generation approach, the transition points between segments tend to exhibit the highest inconsistency. Therefore, in long video generation, we perform the Control Stage and Refinement Stage in a staggered manner. Specifically, the latter half of the preceding structure and the former half of the succeeding structure are used as inputs for a same refinement pass. The refinement stage can seamlessly stitch the two structures together, which ensures a more natural and smoother transition between segments.

Although consistency initialization and staggered refinement have ensured content consistency and smooth transitions between segments, if the motion trend of video structures is not coherent, it will be impossible to combine them into a reasonable long video. Thus, we propose a coherent

Table 2: **Subjective Evaluation Results.** Each model generates videos using the top 100 prompts from Vbench. The videos were evaluated by 30 users, with each video being rated as good, normal, or bad on three dimensions.

Method	Coherence			Text-Match			Visual Quality		
	Bad↓	Normal~	Good↑	Bad↓	Normal~	Good↑	Bad↓	Normal~	Good↑
AnimateDiff-Lightning	0.37	0.42	0.21	<b>0.06</b>	0.51	0.43	0.29	0.51	0.20
Modelscope T2V	0.14	0.48	0.38	0.21	0.53	0.26	0.34	0.45	0.21
Lavie	0.11	0.46	0.43	0.24	0.46	0.30	0.32	0.49	0.19
<b>ConFiner</b> w/ Lavie	0.08	0.43	0.49	0.08	0.48	<b>0.44</b>	0.13	0.36	<b>0.51</b>
<b>ConFiner</b> w/ Modelscope	<b>0.07</b>	0.42	<b>0.51</b>	0.08	0.50	0.42	<b>0.09</b>	0.41	0.50

Table 3: **Ablation Study of Inference Steps of the Refinement Stage.** In the refinement stage, more refinement steps can incorporate more spatio-temporal details. As the refinement steps increase from 5 to 20, all metrics show improvement. However, excessive steps may undermine the control expert’s influence to the final video. Some metrics experience a decline when the steps increase from 20 to 100.

Method	Refinement Steps	Subject Consistency↑	Motion Smoothness↑	Aesthetic Quality ↑	Imaging Quality ↑
<b>ConFiner</b> w/ Lavie	5	0.993	0.991	0.702	0.734
<b>ConFiner</b> w/ Lavie	10	0.994	0.991	0.695	0.733
<b>ConFiner</b> w/ Lavie	20	0.994	0.991	0.709	<b>0.744</b>
<b>ConFiner</b> w/ Lavie	50	0.994	0.990	<b>0.712</b>	0.738
<b>ConFiner</b> w/ Lavie	100	0.994	0.990	0.710	0.735
<b>ConFiner</b> w/ Modelscope	5	0.994	0.991	0.700	0.731
<b>ConFiner</b> w/ Modelscope	10	0.994	0.991	0.697	0.734
<b>ConFiner</b> w/ Modelscope	20	0.994	0.991	0.703	0.734
<b>ConFiner</b> w/ Modelscope	50	0.994	0.991	0.707	<b>0.737</b>
<b>ConFiner</b> w/ Modelscope	100	0.994	0.991	<b>0.708</b>	<b>0.737</b>

Table 4: Comparison of Training and Inference Time.

Time Cost	ConFiner	Lavie	Animate Diffusion	Modelscope
Training	0	> 100× <i>A100 day</i>	> 100× <i>A100 day</i>	> 100× <i>A100 day</i>
Inference	≈5S	>1min	>1min	>1min

guidance to promote the motion trend of new segment to follow the preceding segment. In video generation, predicted noises affect the direction of generation and determine the motion trend. So we generate each structure one by one, using noises of the previous segments to guide the subsequent structure. Specifically, during the sampling process, we use the gradient of the L2 loss to guide the sampling direction. The L2 loss is calculated between the predicted noise of the current segment and the noise in the previous segment. The guided noise is calculated as follows:

$$\epsilon_t^{S_2} = \hat{\epsilon}_t^{S_2} - \gamma \nabla_{\hat{\epsilon}_t^{S_2}} \|\hat{\epsilon}_t^{S_2} - \epsilon_t^{S_1}\|^2 \quad (12)$$

where  $\hat{\epsilon}_t^{S_2}$  represents the noise of current segment predicted by denoising model at timestep  $t$ ,  $\epsilon_t^{S_1}$  is the noise of former segment at timestep  $t$  and  $\gamma$  is a constant.

In this way, coherent guidance can make the noise of the

two segments similar, which allows the motion trend of the latter segment to inherit that of the previous segment. Additionally, coherence guidance also reduces the pixel distance between noises of two segments, which can help maintain content consistency between segments.

## Experiments

In the experiment, we selected AnimateDiff-Lightning (Lin and Yang 2024) as control expert, and Stable Diffusion 1.5 (Rombach et al. 2022) as the spatial expert. For the temporal expert, we opted for two open-source models, lavie (Wang et al. 2023c) and modelscope (Wang et al. 2023b).

### Objective Evaluation

For objective evaluation experiments, we utilized the cutting-edge benchmark, Vbench (Huang et al. 2023). Vbench provides 800 prompts that test various capabilities of video generation models. In our experiments, each model was tasked with generating 800 videos using these prompts, and the resulting videos were assessed using four metrics to evaluate their Temporal Quality and Frame-wise Quality.

For Temporal Quality Metrics, we use Subject Consistency and Motion Smoothness. For Frame-wise Quality Metrics, we use Aesthetic Quality and Imaging Quality.

In this experiment, we employed AnimateDiff-Lightning, Lavie, and modelscope T2V to generate over total timesteps

Table 5: **Ablation Study of  $T_e$ .** In most cases, as  $T_e$  increases, the temporal metric decreases and the imaging quality improves. However, when the control stage involves only 4 steps, too high values of  $T_e$  (such as 300 or 500) can lead to imaging collapse.

Method	Control Stage Steps	$T_e$	Subject Consistency $\uparrow$	Motion Smoothness $\uparrow$	Aesthetic Quality $\uparrow$	Imaging Quality $\uparrow$
ConFiner w/ Lavie	4	50	<b>0.993</b>	<b>0.991</b>	0.703	0.733
ConFiner w/ Lavie	4	100	<b>0.993</b>	0.990	0.702	0.737
ConFiner w/ Lavie	4	200	0.992	0.989	<b>0.710</b>	<b>0.744</b>
ConFiner w/ Lavie	4	300	0.978	0.986	0.383	0.303
ConFiner w/ Lavie	4	500	0.967	0.983	0.338	0.265
ConFiner w/ Modelscope	4	50	<b>0.995</b>	<b>0.991</b>	0.701	0.733
ConFiner w/ Modelscope	4	100	0.994	<b>0.991</b>	0.698	0.733
ConFiner w/ Modelscope	4	200	0.994	0.990	<b>0.712</b>	<b>0.736</b>
ConFiner w/ Modelscope	4	300	0.990	0.987	0.560	0.429
ConFiner w/ Modelscope	4	500	0.993	0.992	0.513	0.370
ConFiner w/ Lavie	8	50	<b>0.994</b>	<b>0.991</b>	0.708	0.741
ConFiner w/ Lavie	8	100	0.993	0.990	0.706	0.739
ConFiner w/ Lavie	8	200	0.991	0.989	0.716	0.742
ConFiner w/ Lavie	8	300	0.983	0.985	0.718	0.744
ConFiner w/ Lavie	8	500	0.978	0.980	<b>0.721</b>	<b>0.751</b>
ConFiner w/ Modelscope	8	50	<b>0.994</b>	<b>0.991</b>	0.708	0.740
ConFiner w/ Modelscope	8	100	0.994	<b>0.991</b>	0.707	0.739
ConFiner w/ Modelscope	8	200	0.993	0.990	0.716	0.742
ConFiner w/ Modelscope	8	300	0.992	0.989	0.720	0.747
ConFiner w/ Modelscope	8	500	0.991	0.987	<b>0.727</b>	<b>0.752</b>

of 10, 20, 50, and 100. We then utilize our ConFiner to conduct generation with 9(4+5) and 18(8+10) timesteps, where  $T_e$  is set to 100. All evaluation results are presented in table 1. Each individual experiment can be completed in 3-5 hours on a single RTX 4090. In each experiment, we repeated for five times with different random seeds.

### Subjective Evaluation

In our subjective evaluation, we employed our ConFiner with 18 inference steps to generate videos using the top 100 prompts from Vbench. These videos were evaluated alongside those generated by Animate-Diff Lightning, Modelscope T2V, and Lavie with 50-step inference, by 30 users. Users rated each video across three dimensions: coherence, text-match, and visual quality, each dimension being categorized into three levels: good, normal, and bad. The scoring results are shown in table 2.

### Comparison of Computation Efficiency

In this section, we compare the training and inference cost of our ConFiner with other video diffusion models. The results are shown in table 4.

### Ablation Study on Control and Refinement Level

As eq. (6), we apply noise for  $T_e$  steps to the videos generated during the control stage to create optimization space for the refinement stage. A larger  $T_e$  value increases the impact of the refinement stage. For the four settings same as objective experiment, we set  $T_e$  to 50, 100, 200, 300, and 500, with other experimental settings consistent. The performance comparison is shown in table 5.

Furthermore, in previous experiments, when 4-step rapid sampling was used in the control stage, the refinement stage consistently utilized a total of 5 inference steps. To examine the impact of the number of refinement steps, while keeping  $T_e$  at 100, we used Modelscope T2V and Lavie as our temporal experts, selecting total inference steps of 5, 10, 20, 50, and 100 for the refinement stage. The resulting performance metrics are presented in table 3.

## Conclusion

In this paper, we introduce ConFiner, a training-free framework that can generate high-quality videos with chain of diffusion experts. It decomposes video generation into three components: structure control, spatial refinement and temporal refinement. Each component is handled by a off-the-shelf expert that specializes in this task. Additionally, we propose coordinated denoising to enable two expert cooperate when denoising. We also design ConFiner-Long framework to generate long coherent videos. Experimental results confirm that our ConFiner enhances the aesthetics and coherence of generated videos while reducing sampling time significantly. And our ConFiner-Long can generate consistent and coherent videos with up to 600 frames. Our approach paves the way for cost-effective new possibilities in filmmaking, animation production, and video editing.

## References

Blattmann, A.; Dockhorn, T.; Kulal, S.; Mendeleevitch, D.; Kilian, M.; Lorenz, D.; Levi, Y.; English, Z.; Voleti, V.; Letts, A.; et al. 2023. Stable video diffusion: Scaling la-

- tent video diffusion models to large datasets. *arXiv preprint arXiv:2311.15127*.
- Cao, Y.; Li, S.; Liu, Y.; Yan, Z.; Dai, Y.; Yu, P. S.; and Sun, L. 2023. A comprehensive survey of ai-generated content (aigc): A history of generative ai from gan to chatgpt. *arXiv preprint arXiv:2303.04226*.
- Esser, P.; Chiu, J.; Atighehchian, P.; Granskog, J.; and Germanidis, A. 2023. Structure and content-guided video synthesis with diffusion models. In *Proceedings of the IEEE/CVF International Conference on Computer Vision*, 7346–7356.
- Gu, J.; Wang, S.; Zhao, H.; Lu, T.; Zhang, X.; Wu, Z.; Xu, S.; Zhang, W.; Jiang, Y.-G.; and Xu, H. 2023. Reuse and diffuse: Iterative denoising for text-to-video generation. *arXiv preprint arXiv:2309.03549*.
- Ho, J.; Chan, W.; Saharia, C.; Whang, J.; Gao, R.; Gritsenko, A.; Kingma, D. P.; Poole, B.; Norouzi, M.; Fleet, D. J.; et al. 2022a. Imagen video: High definition video generation with diffusion models. *arXiv preprint arXiv:2210.02303*.
- Ho, J.; Chan, W.; Saharia, C.; Whang, J.; Gao, R.; Gritsenko, A.; Kingma, D. P.; Poole, B.; Norouzi, M.; Fleet, D. J.; et al. 2022b. Imagen video: High definition video generation with diffusion models. *arXiv preprint arXiv:2210.02303*.
- Ho, J.; Salimans, T.; Gritsenko, A.; Chan, W.; Norouzi, M.; and Fleet, D. J. 2022c. Video diffusion models. *Advances in Neural Information Processing Systems*, 35: 8633–8646.
- Huang, Z.; He, Y.; Yu, J.; Zhang, F.; Si, C.; Jiang, Y.; Zhang, Y.; Wu, T.; Jin, Q.; Chanpaisit, N.; et al. 2023. Vbench: Comprehensive benchmark suite for video generative models. *arXiv preprint arXiv:2311.17982*.
- Khachatryan, L.; Movsisyan, A.; Tadevosyan, V.; Henschel, R.; Wang, Z.; Navasardyan, S.; and Shi, H. 2023. Text2video-zero: Text-to-image diffusion models are zero-shot video generators. In *Proceedings of the IEEE/CVF International Conference on Computer Vision*, 15954–15964.
- Lin, C.-H.; Gao, J.; Tang, L.; Takikawa, T.; Zeng, X.; Huang, X.; Kreis, K.; Fidler, S.; Liu, M.-Y.; and Lin, T.-Y. 2023. Magic3d: High-resolution text-to-3d content creation. In *Proceedings of the IEEE/CVF Conference on Computer Vision and Pattern Recognition*, 300–309.
- Lin, S.; and Yang, X. 2024. AnimateDiff-Lightning: Cross-Model Diffusion Distillation. *arXiv preprint arXiv:2403.12706*.
- Ma, X.; Wang, Y.; Jia, G.; Chen, X.; Liu, Z.; Li, Y.-F.; Chen, C.; and Qiao, Y. 2024. Latte: Latent diffusion transformer for video generation. *arXiv preprint arXiv:2401.03048*.
- Mittal, G.; Engel, J.; Hawthorne, C.; and Simon, I. 2021. Symbolic music generation with diffusion models. *arXiv preprint arXiv:2103.16091*.
- Nichol, A. Q.; and Dhariwal, P. 2021. Improved denoising diffusion probabilistic models. In *International conference on machine learning*, 8162–8171. PMLR.
- Poole, B.; Jain, A.; Barron, J. T.; and Mildenhall, B. 2022. Dreamfusion: Text-to-3d using 2d diffusion. *arXiv preprint arXiv:2209.14988*.
- Qiu, H.; Xia, M.; Zhang, Y.; He, Y.; Wang, X.; Shan, Y.; and Liu, Z. 2023. Freenoise: Tuning-free longer video diffusion via noise rescheduling. *arXiv preprint arXiv:2310.15169*.
- Rombach, R.; Blattmann, A.; Lorenz, D.; Esser, P.; and Ommer, B. 2022. High-resolution image synthesis with latent diffusion models. In *Proceedings of the IEEE/CVF conference on computer vision and pattern recognition*, 10684–10695.
- Saharia, C.; Chan, W.; Saxena, S.; Li, L.; Whang, J.; Denton, E. L.; Ghasemipour, K.; Gontijo Lopes, R.; Karagol Ayan, B.; Salimans, T.; et al. 2022. Photorealistic text-to-image diffusion models with deep language understanding. *Advances in neural information processing systems*, 35: 36479–36494.
- Song, J.; Meng, C.; and Ermon, S. 2020. Denoising diffusion implicit models. *arXiv preprint arXiv:2010.02502*.
- Wang, F.-Y.; Chen, W.; Song, G.; Ye, H.-J.; Liu, Y.; and Li, H. 2023a. Gen-l-video: Multi-text to long video generation via temporal co-denoising. *arXiv preprint arXiv:2305.18264*.
- Wang, J.; Yuan, H.; Chen, D.; Zhang, Y.; Wang, X.; and Zhang, S. 2023b. Modelscope text-to-video technical report. *arXiv preprint arXiv:2308.06571*.
- Wang, X.; Li, X.; and Chen, Z. 2024. CoNo: Consistency Noise Injection for Tuning-free Long Video Diffusion. *arXiv preprint arXiv:2406.05082*.
- Wang, Y.; Chen, X.; Ma, X.; Zhou, S.; Huang, Z.; Wang, Y.; Yang, C.; He, Y.; Yu, J.; Yang, P.; et al. 2023c. Lavie: High-quality video generation with cascaded latent diffusion models. *arXiv preprint arXiv:2309.15103*.
- Wu, J.; Gan, W.; Chen, Z.; Wan, S.; and Lin, H. 2023. Ai-generated content (aigc): A survey. *arXiv preprint arXiv:2304.06632*.
- Xing, Z.; Feng, Q.; Chen, H.; Dai, Q.; Hu, H.; Xu, H.; Wu, Z.; and Jiang, Y.-G. 2023. A survey on video diffusion models. *arXiv preprint arXiv:2310.10647*.
- Zhang, C.; Zhang, C.; Zheng, S.; Qiao, Y.; Li, C.; Zhang, M.; Dam, S. K.; Thwal, C. M.; Tun, Y. L.; Huy, L. L.; et al. 2023a. A complete survey on generative ai (aigc): Is chatgpt from gpt-4 to gpt-5 all you need? *arXiv preprint arXiv:2303.11717*.
- Zhang, D. J.; Wu, J. Z.; Liu, J.-W.; Zhao, R.; Ran, L.; Gu, Y.; Gao, D.; and Shou, M. Z. 2023b. Show-1: Marrying pixel and latent diffusion models for text-to-video generation. *arXiv preprint arXiv:2309.15818*.
- Zhang, S.; Wang, J.; Zhang, Y.; Zhao, K.; Yuan, H.; Qin, Z.; Wang, X.; Zhao, D.; and Zhou, J. 2023c. I2vgen-xl: High-quality image-to-video synthesis via cascaded diffusion models. *arXiv preprint arXiv:2311.04145*.